Electronic Supplementary Material (ESI) for RSC Advances.

Supporting information

An investigation of the metabolic activity, isozyme contribution, species differences and potential drug-drug interactions of PI-103, and the identification of efflux transporters for PI-103-*O*-glucuronide in HeLa1A9 cells

Li Gao,[ab] Zifei Qin,*[ab] Beibei Zhang,[ab] Zhao Yin,[ab] Xiaojian Zhang,[ab] and Jing Yang,*[ab]

[a] *Department of Pharmacy, the First Affiliated Hospital of Zhengzhou University, Zhengzhou 450052, China;*

[b] *Henan Key Laboratory of Precision Clinical Pharmacy, Zhengzhou University, Zhengzhou 450052, China;*

*** Corresponding authors**

E-mail: qzf1989@163.com (Zifei Qin); jingyang_0101@163.com (Jing Yang); Tel.: +86-371-66913423;

Figure legends

Figure S1 Kinetic profiles for metabolic activities of PI-103 in HLM and HIM. (A) Mono-oxidation of PI-103 in HLM; (B) Mono-oxidation of PI-103 in HIM; (C) Mono-glucuronidation of PI-103 in HLM; (D) Mono-glucuronidation of PI-103 in HIM; In each panel, the insert figure showed the corresponding Eadie-Hofstee plot. All experiments were performed in triplicate.

Figure S2 Metabolic rates of PI-103 by expressed CYP and UGT enzymes at 1 and 10 μM. (A) Metabolic rates for mono-oxidation of PI-103 by twelve expressed CYP isoforms; (B) Metabolic rates for mono-glucuronidation of PI-103 by thirteen expressed UGT isoforms; All experiments were performed in triplicate. N.D.: not detected; N.A.: due to the concentration under the limit of quantification, it was unavailable to determine the kinetic parameters.

Figure S3 Kinetic profiles for mono-oxidation of PI-103 in five expressed CYP enzymes. (A) Kinetic profiles by CYP1A1; (B) Kinetic profiles by CYP1A2; (C) Kinetic profiles by CYP1B1; (D) Kinetic profiles by CYP3A4; (E) Kinetic profiles by CYP3A5; In each panel, the insert figure showed the corresponding Eadie-Hofstee plot. All experiments were performed in triplicate.

Figure S4 Kinetic profiles for mono-glucuronidation of PI-103 in six expressed UGT enzymes. (A) Kinetic profiles by UGT1A1; (B) Kinetic profiles by UGT1A3; (C) Kinetic profiles by UGT1A7; (D) Kinetic profiles by UGT1A8; (E) Kinetic profiles by UGT1A9; (E) Kinetic profiles by UGT1A10; In each panel, the insert figure showed the corresponding Eadie-Hofstee plot. All experiments were performed in triplicate.

Figure S5 Inhibitory effects of several inhibitors on the metabolic activities of PI-103 in HLM. (A) Inhibitory effects on mono-oxidation of PI-103; (B) Inhibitory effects on mono-glucuronidation of PI-103; All experiments were performed in triplicate. (*, # Compared with the control values of M1 and M2 in HLM, respectively. *, # $p < 0.05$, **, ## $p < 0.01$, ***, ### $p < 0.001$)

Figure S6 Correlation analysis for the metabolic activities of PI-103 in a bank of individual HLM (n = 12). (A) Correlation analysis between PI-103-oxidation and phenacetin-N-deacetylation; (B) Correlation analysis between PI-103-oxidation and

nifedipine-oxidation; (C) Correlation analysis between PI-103-*O*-glucuronidation and β-estradiol-3-O-glucuronidation; (D) Correlation analysis between PI-103-*O*-glucuronidation and propofol-O-glucuronidation; All experiments were performed in triplicate. (* $p < 0.05$, ** $p < 0.01$, *** $p < 0.001$).

Figure S7 Kinetic profiles for mono-oxidation of PI-103 by various types of microsomes. (A) Kinetic profiles by dog liver microsomes (DLM); (B) Kinetic profiles by mice liver microsomes (MLM); (C) Kinetic profiles by rat liver microsomes (RLM); (D) Kinetic profiles by mini-pig liver microsomes (MpLM); In each panel, the insert figure showed the corresponding Eadie-Hofstee plot. All experiments were performed in triplicate.

Figure S8 Kinetic profiles for mono-glucuronidation of PI-103 by various types of microsomes. (A) Kinetic profiles by dog liver microsomes (DLM); (B) Kinetic profiles by mice liver microsomes (MLM); (C) Kinetic profiles by rat liver microsomes (RLM); (D) Kinetic profiles by mini-pig liver microsomes (MpLM); In each panel, the insert figure showed the corresponding Eadie-Hofstee plot. All experiments were performed in triplicate.

Figure S9 UGT1A9-mediated PI-103-O-glucuronidation in HeLa1A9 cells. (A) Excreted PI-103-O-glucuronide in extracellular solution at two concentrations of propofol (2.5 and 5 μM); (B) Excreted rates of PI-103-O-glucuronide at different concentrations (2.5 and 5 μM); All experiments were performed in triplicate. Data were presented as mean ± SD. * $p < 0.05$, ** $p < 0.01$ or *** $p < 0.001$ compared with that of PI-103 (2.5 μM).

Figure S10 Concentration-dependent inhibition evaluation of PI-103 towards several expressed CYP enzymes. (A) Concentration-dependent plot towards CYP1A1-mediated ethoxyresorufin-deethylation; (B) Concentration-dependent plot towards CYP1A2-mediated phenacetin-*N*-deacetylation; (C) Concentration-dependent plot towards CYP2B6-mediated bupropion-hydroxylation; (D) Concentration-dependent plot towards CYP2C9-mediated tolbutamide-4-hydroxylation; (E) Concentration-dependent plot towards CYP2C19-mediated mephenytoin-4-hydroxylation; (F) Concentration-dependent plot towards CYP2E1-mediated chlorzoxazone-6-

hydroxylation; All experiments were performed in triplicate. Data were presented as mean ± SD.

Figure S11 Concentration-dependent inhibition evaluation of PI-103 against several expressed UGT enzymes. (A) Concentration-dependent plot against UGT1A3-mediated 4-MU-glucuronidation; (B) Concentration-dependent plot against UGT1A6-mediated 4-MU-glucuronidation; (C) Concentration-dependent plot against UGT1A7-mediated 4-MU-glucuronidation; (D) Concentration-dependent plot against UGT1A9-mediated propofol-glucuronidation; (E) Concentration-dependent plot against UGT2B7-mediated 4-MU glucuronidation; All experiments were performed in triplicate. Data were presented as mean ± SD.

Table list

Table S1 Detailed UHPLC and MRM conditions information for quantification of the metabolites of specific substrates

Table S2 Selection of inhibition type of PI-103 towards six CYPs and five UGTs isozymes

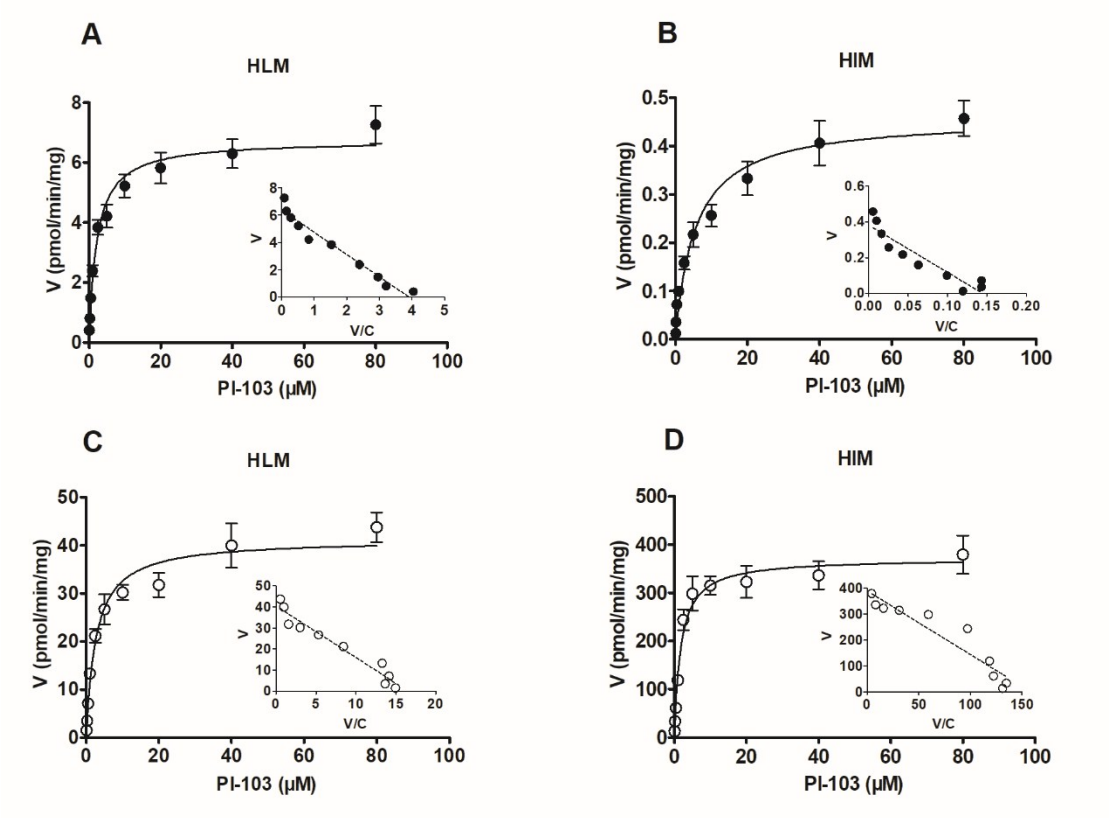
A
HLM
V (pmol/min/mg)
PI-103 (μM)
V
V/C
B
HIM
V (pmol/min/mg)
PI-103 (μM)
V
V/C
C
HLM
V (pmol/min/mg)
PI-103 (μM)
V
V/C
D
HIM
V (pmol/min/mg)
PI-103 (μM)
V
V/C

Figure S1

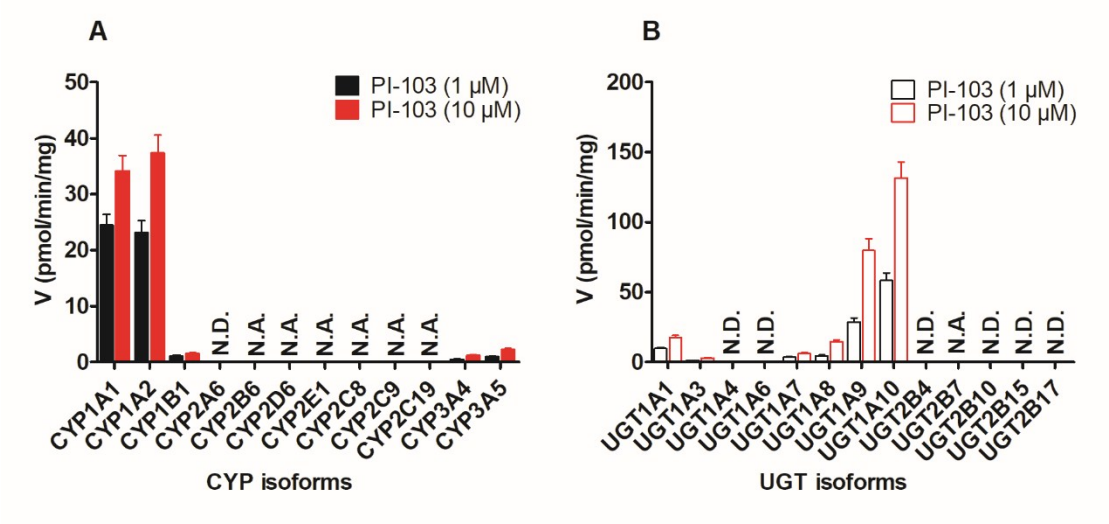
A
PI-103 (1 μM)
PI-103 (10 μM)
V (pmol/min/mg)
50
40
30
20
10
0
N.D.
N.A.
N.A.
N.A.
N.A.
N.A.
N.A.
CYP1A1
CYP1A2
CYP1B1
CYP2A6
CYP2B6
CYP2D6
CYP2E1
CYP2C8
CYP2C9
CYP2C19
CYP3A4
CYP3A5
CYP isoforms
B
PI-103 (1 μM)
PI-103 (10 μM)
V (pmol/min/mg)
200
150
100
50
0
N.D.
N.D.
N.D.
N.A.
N.D.
N.D.
N.D.
UGT1A1
UGT1A3
UGT1A4
UGT1A6
UGT1A7
UGT1A8
UGT1A9
UGT1A10
UGT2B4
UGT2B7
UGT2B10
UGT2B15
UGT2B17
UGT isoforms

Figure S2

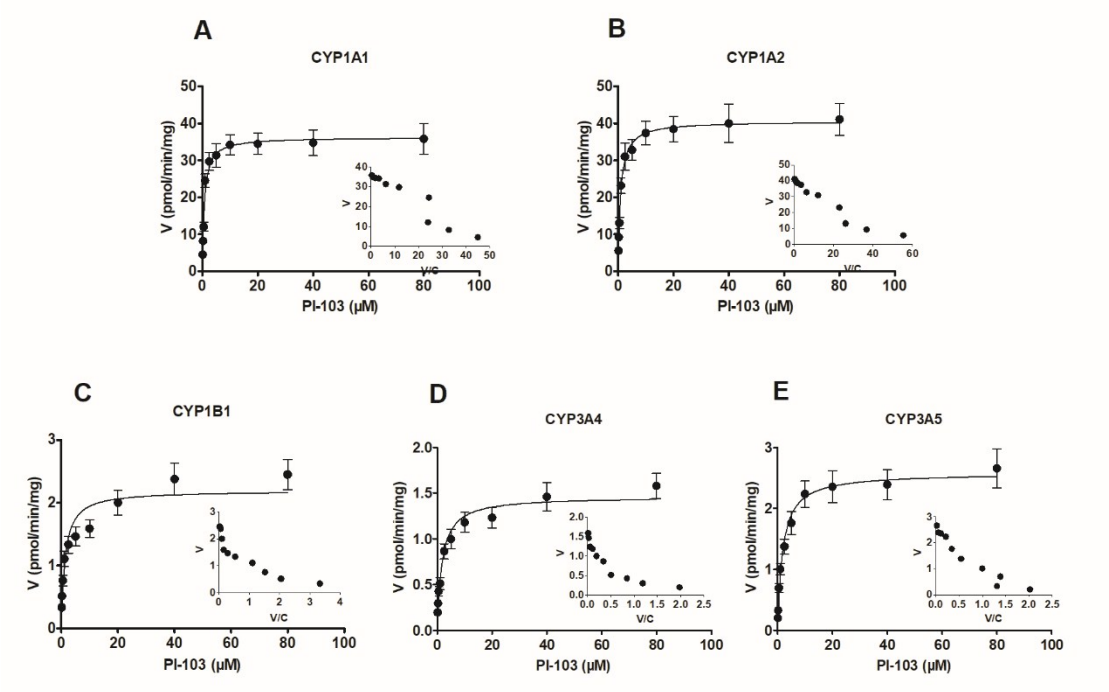
A
CYP1A1
V (pmol/min/mg)
PI-103 (μM)
V
V/C
B
CYP1A2
V (pmol/min/mg)
PI-103 (μM)
V
V/C
C
CYP1B1
V (pmol/min/mg)
PI-103 (μM)
V
V/C
D
CYP3A4
V (pmol/min/mg)
PI-103 (μM)
V
V/C
E
CYP3A5
V (pmol/min/mg)
PI-103 (μM)
V
V/C

Figure S3

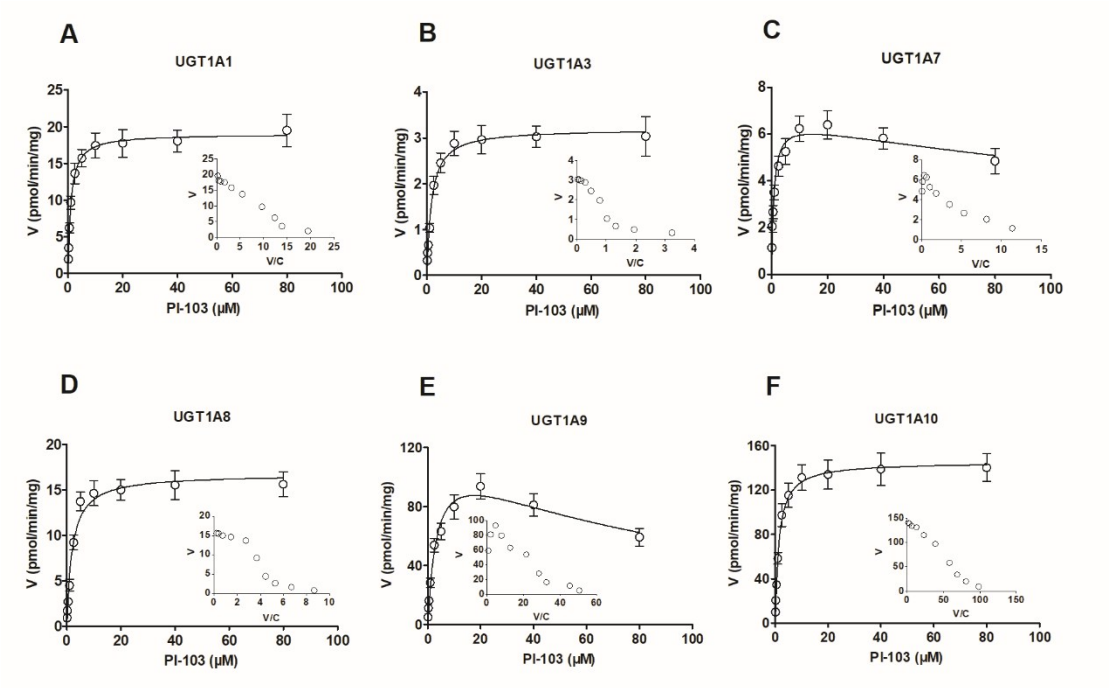
A
UGT1A1
V (pmol/min/mg)
PI-103 (μM)
V
V/C
B
UGT1A3
V (pmol/min/mg)
PI-103 (μM)
V
V/C
C
UGT1A7
V (pmol/min/mg)
PI-103 (μM)
V
V/C
D
UGT1A8
V (pmol/min/mg)
PI-103 (μM)
V
V/C
E
UGT1A9
V (pmol/min/mg)
PI-103 (μM)
V
V/C
F
UGT1A10
V (pmol/min/mg)
PI-103 (μM)
V
V/C

Figure S4

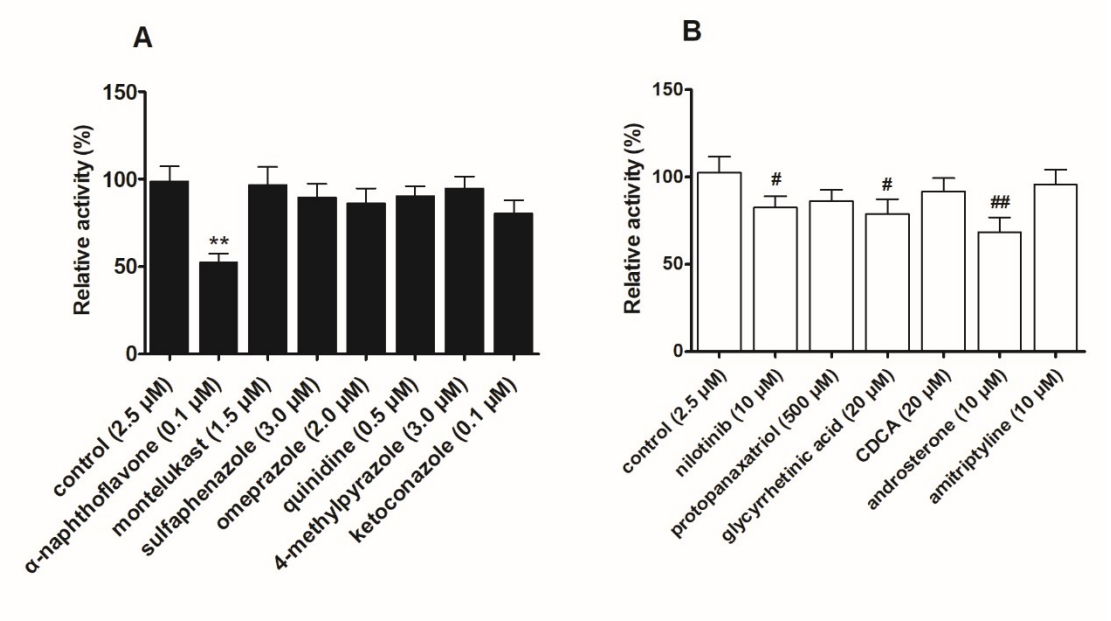
A
Relative activity (%)
150
100
50
0
**
control (2.5 μM)
α-naphthoflavone (0.1 μM)
montelukast (1.5 μM)
sulfaphenazole (3.0 μM)
omeprazole (2.0 μM)
quinidine (0.5 μM)
4-methylpyrazole (3.0 μM)
ketoconazole (0.1 μM)
B
Relative activity (%)
150
100
50
0
#
#
##
control (2.5 μM)
nilotinib (10 μM)
protopanaxatriol (500 μM)
glycyrrhetinic acid (20 μM)
CDCA (20 μM)
androsterone (10 μM)
amitriptyline (10 μM)

Figure S5

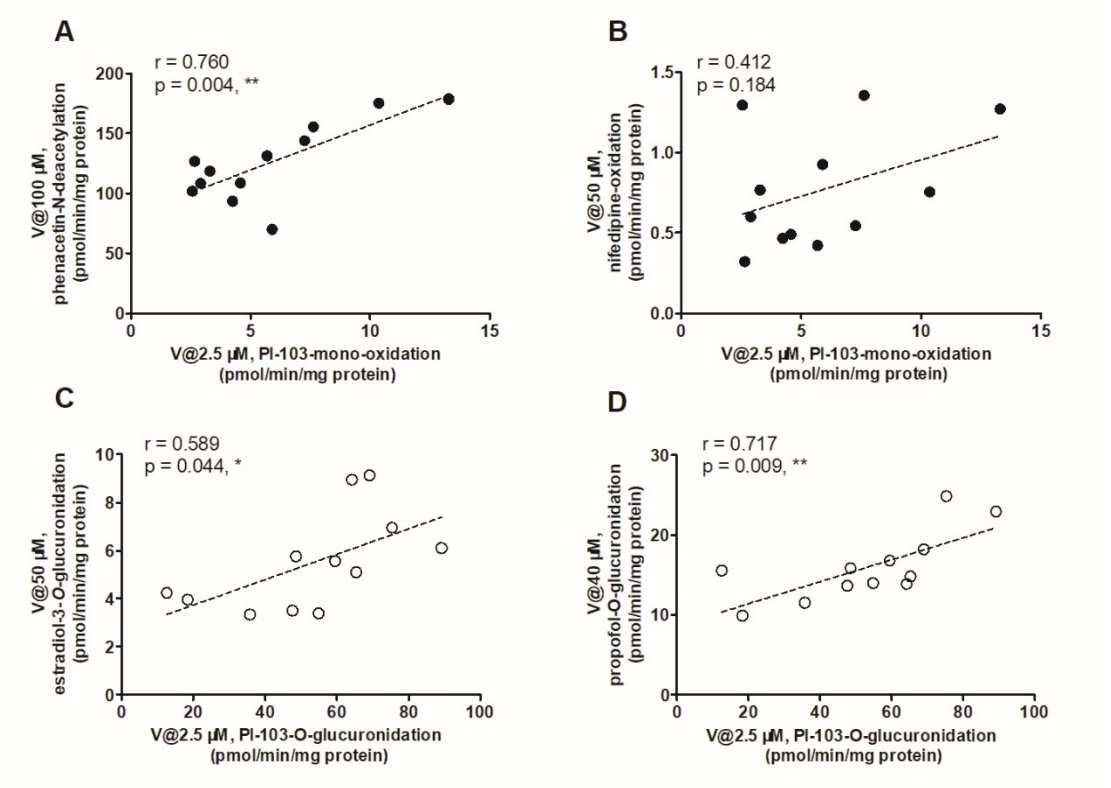
A
r = 0.760
p = 0.004, **
V@100 µM, phenacetin-N-deacetylation (pmol/min/mg protein)
V@2.5 µM, PI-103-mono-oxidation (pmol/min/mg protein)
B
r = 0.412
p = 0.184
V@50 µM, nifedipine-oxidation (pmol/min/mg protein)
V@2.5 µM, PI-103-mono-oxidation (pmol/min/mg protein)
C
r = 0.589
p = 0.044, *
V@50 µM, estradiol-3-O-glucuronidation (pmol/min/mg protein)
V@2.5 µM, PI-103-O-glucuronidation (pmol/min/mg protein)
D
r = 0.717
p = 0.009, **
V@40 µM, propofol-O-glucuronidation (pmol/min/mg protein)
V@2.5 µM, PI-103-O-glucuronidation (pmol/min/mg protein)

Figure S6

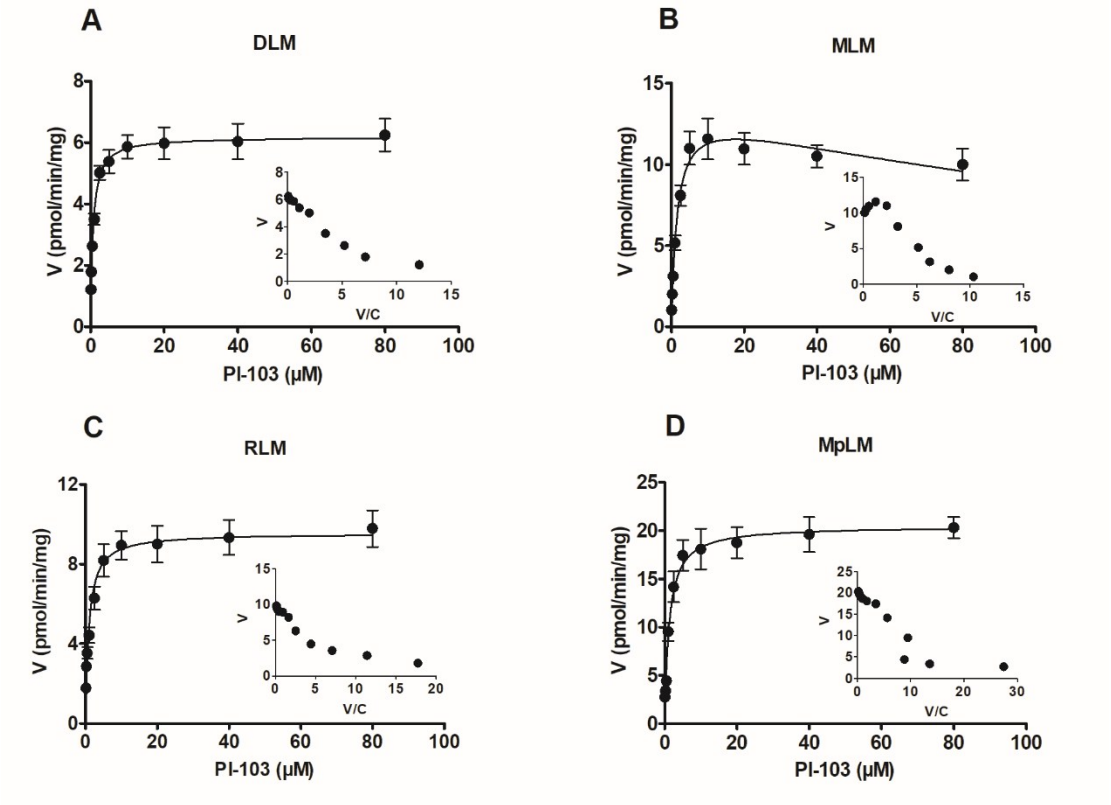
A
DLM
V (pmol/min/mg)
PI-103 (μM)
V
V/C
B
MLM
V (pmol/min/mg)
PI-103 (μM)
V
V/C
C
RLM
V (pmol/min/mg)
PI-103 (μM)
V
V/C
D
MpLM
V (pmol/min/mg)
PI-103 (μM)
V
V/C

Figure S7

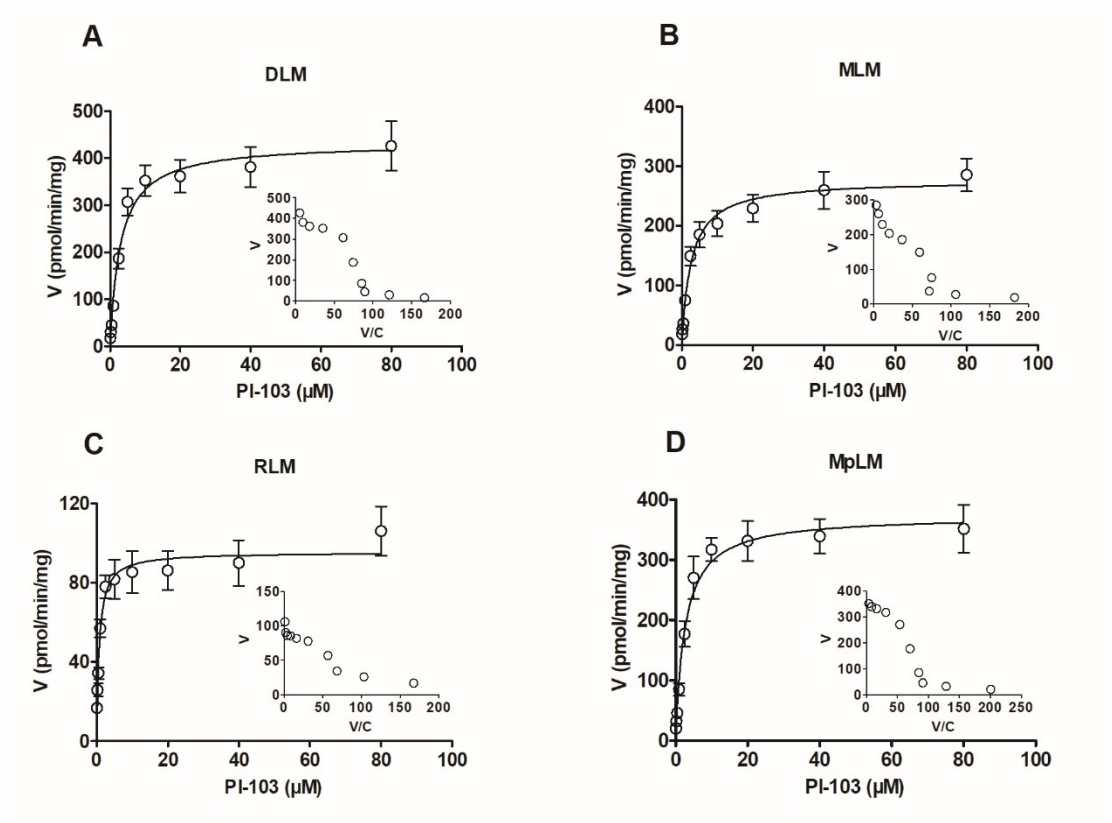
A
DLM
V (pmol/min/mg)
PI-103 (μM)
V
V/C
B
MLM
V (pmol/min/mg)
PI-103 (μM)
V
V/C
C
RLM
V (pmol/min/mg)
PI-103 (μM)
V
V/C
D
MpLM
V (pmol/min/mg)
PI-103 (μM)
V
V/C

Figure S8

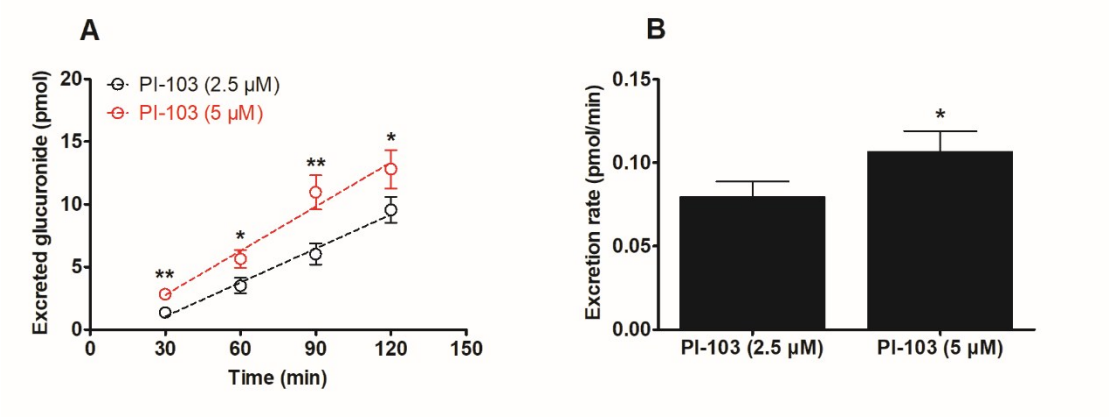
A
PI-103 (2.5 μM)
PI-103 (5 μM)
Excreted glucuronide (pmol)
20
15
10
5
0
0
30
60
90
120
150
Time (min)
**
*
**
*
B
Excretion rate (pmol/min)
0.15
0.10
0.05
0.00
*
PI-103 (2.5 μM)
PI-103 (5 μM)

Figure S9

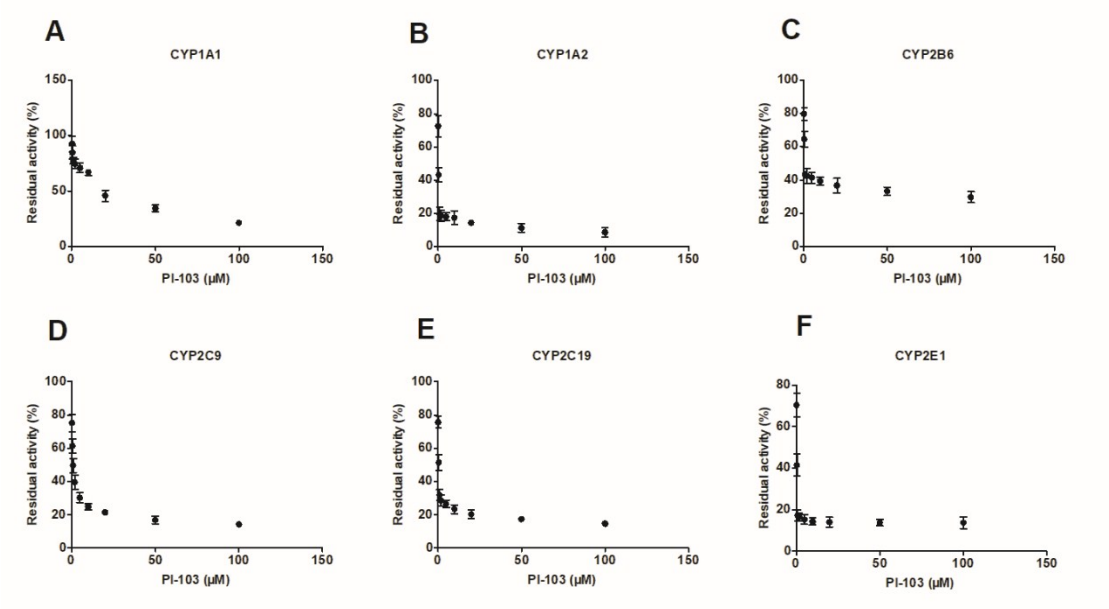
A
CYP1A1
Residual activity (%)
PI-103 (μM)
B
CYP1A2
Residual activity (%)
PI-103 (μM)
C
CYP2B6
Residual activity (%)
PI-103 (μM)
D
CYP2C9
Residual activity (%)
PI-103 (μM)
E
CYP2C19
Residual activity (%)
PI-103 (μM)
F
CYP2E1
Residual activity (%)
PI-103 (μM)

Figure S10

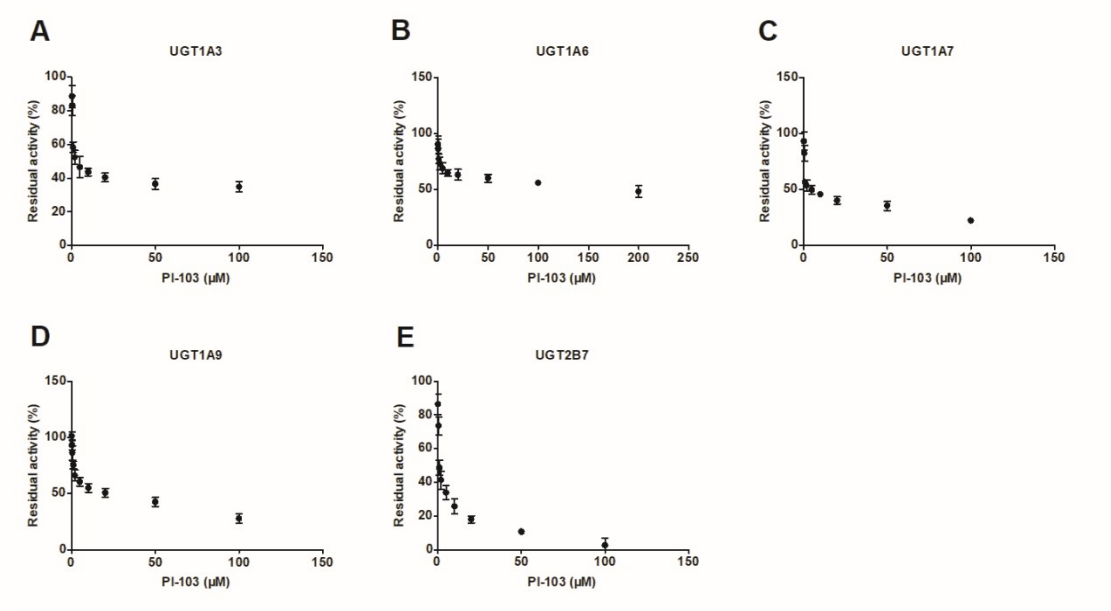
A
UGT1A3
Residual activity (%)
PI-103 (μM)
B
UGT1A6
Residual activity (%)
PI-103 (μM)
C
UGT1A7
Residual activity (%)
PI-103 (μM)
D
UGT1A9
Residual activity (%)
PI-103 (μM)
E
UGT2B7
Residual activity (%)
PI-103 (μM)

Figure S11

Table S1 Detailed UHP LC and MRM conditions information for quantification of the metabolites of specific substrates

Enzymes	Substrates	Metabolites	UHPLC conditions	t_R (min)	MRM Conditions			
					Parent (m/z)	Daughters (m/z)	Cone (V)	Collision (V)
Human CYP enzymes								
CYP1A1	ethoxyresorufin	resorufin	0-0.4 min, 10%B;	1.45 (+)	214.050	186.020	60	25
CYP1A2	phenacetin	paracetamol	0.4-1.4 min, 10%-	0.91 (+)	152.071	110.050	50	15
CYP2A6	coumarin	7-hydroxycoumarin	95%B; 1.4-1.6 min,	1.42 (+)	163.040	107.030	40	20
CYP2B6	bupropion	hydroxybupropion	95%B; 1.6-1.8 min,	1.37 (+)	256.110	238.100	20	10
CYP2C8	paclitaxel	6α-hydroxy-paclitaxel	95%-10%B; 1.8-2.0	1.75 (+)	870.334	105.200	30	45
CYP2C9	tolbutamide	4-hydroxytolbutamide	min, 10%B;	1.50 (+)	287.107	89.300	30	40
CYP2C19	*S*-mephenytoin	4-hydroxymephenytoin		1.41 (+)	235.108	150.100	40	20
CYP2E1	chlorzoxazone	6-hydroxychlorzoxazone	0.3 ml/min	1.36 (-)	183.980	119.900	40	20
CYP3A4	nifedipine	oxidized nifedipine	35 °C	1.76 (+)	345.109	284.100	60	30
CYP3A5	nifedipine	oxidized nifedipine		1.76 (+)	345.109	284.100	60	30
Human UGT enzymes								
UGT1A1	β-estradiol	β-estradiol-3-glucuronide	0-0.4 min, 10%B;	1.48 (-)	447.202	113.200	50	20
UGT1A3	4-MU	4-MU-glucuronide	0.4-1.4 min, 10%-	1.30 (-)	351.072	175.050	30	25
UGT1A4	TFP	TFP-*N*-glucuronide	95%B; 1.4-1.6 min,	1.58 (+)	584.204	408.210	50	25
UGT1A6	4-MU	4-MU-glucuronide	95%B; 1.6-1.8 min,	1.30 (-)	351.072	175.050	30	25
UGT1A7	4-MU	4-MU-glucuronide	95%-10%B; 1.8-2.0	1.30 (-)	351.072	175.050	30	25
UGT1A8	4-MU	4-MU-glucuronide	min, 10%B;	1.30 (-)	351.072	175.050	30	25
UGT1A9	propofol	propofol-*O*-glucuronide		1.60 (-)	353.160	177.100	50	25
UGT1A10	4-MU	4-MU-glucuronide	0.3 ml/min	1.30 (-)	351.072	175.050	30	25
UGT2B4	4-MU	4-MU-glucuronide	35 °C	1.30 (-)	351.072	175.050	30	25
UGT2B7	4-MU	4-MU-glucuronide		1.30 (-)	351.072	175.050	30	25
UGT2B10	4-MU	4-MU-glucuronide		1.30 (-)	351.072	175.050	30	25
UGT2B15	4-MU	4-MU-glucuronide		1.30 (-)	351.072	175.050	30	25

UGT2B17	4-MU	4-MU-glucuronide	1.30 (-)	351.072	175.050	30	25

Note: 4-MU, 4-methylumbelliferone; TFP, trifluoperazine; (+) and (-) means ESI+ and ESI-, respectively.

Table S2 Selection of inhibition type of PI-103 towards six CYPs and five UGTs isozymes

Isozymes	Substrate	Type of inhibition	K_i (μM)	α	Goodness of fit (R^2)	AIC	SC	Selection
UGT1A3	4-MU	Competitive	0.94±0.27	——	0.9368	-164.81	-162.49	
		Noncompetitive	5.22±0.48	——	0.9689	-176.16	-173.84	
		Mixed-type	2.58±0.84	2.97±1.61	0.9757	-178.09	-175.00	√
UGT1A7	4-MU	Competitive	1.15±0.34	——	0.9242	-143.50	-141.18	
		Noncompetitive	5.64±0.60	——	0.9611	-154.18	-151.86	√
		Mixed-type	3.32±1.37	2.28±1.52	0.9648	-153.76	-150.67	
UGT2B7	4-MU	Competitive	0.75±0.13	——	0.9691	-226.97	-224.66	
		Noncompetitive	1.35±0.15	——	0.9721	-228.62	-226.30	√
		Mixed-type	1.13±0.43	1.66±1.92	0.9726	-226.86	-223.77	
CYP1A2	Phenacetin	Competitive	0.08±0.02	——	0.9288	-102.20	-99.88	
		Noncompetitive	0.38±0.03	——	0.9779	-120.90	-118.58	√
		Mixed-type	0.26±0.10	1.70±0.93	0.9793	-120.01	-116.61	
CYP2B6	Bupropion	Competitive	0.40±0.08	——	0.9594	-217.86	-215.55	
		Noncompetitive	1.44±0.17	——	0.9567	-216.81	-214.49	
		Mixed-type	0.64±0.22	5.09±4.48	0.9673	-219.32	-216.23	√
CYP2C9	Tolbutamide	Competitive	0.24±0.05	——	0.9640	-224.83	-222.51	
		Noncompetitive	0.96±0.06	——	0.9859	-239.83	-237.51	
		Mixed-type	0.56±0.12	2.45±0.94	0.9901	-243.41	-240.32	√
CYP2C19	Mephenytoin	Competitive	0.11±0.04	——	0.8967	-143.75	-141.44	
		Noncompetitive	0.53±0.03	——	0.9848	-174.46	-172.14	√
		Mixed-type	0.68±0.27	0.71±0.37	0.9854	-173.05	-169.96	
CYP2E1	Chlorzoxazone	Competitive	0.06±0.01	——	0.9549	-142.25	-139.94	
		Noncompetitive	0.25±0.01	——	0.9949	-177.37	-175.05	√
		Mixed-type	0.21±0.04	1.33±0.37	0.9953	-176.64	-173.55	

Note: 4-MU, 4-methylumbelliferone.